

Intermingled fractal Arnold tongues

V. Paar and N. Pavin

Department of Physics, Faculty of Science, University of Zagreb, Zagreb, Croatia

(Received 6 March 1997; revised manuscript received 5 September 1997)

We present a pattern of multiply interwoven Arnold tongues in the case of the single-well Duffing oscillator at low dissipation and weak forcing: Strips of $\frac{2}{2}$ Arnold tongues form a truncated fractal structure and the tongue-like regions in between are filled by finely intermingled fractal-like $\frac{1}{1}$ and $\frac{3}{3}$ Arnold tongues, which are fat fractals characterized by the uncertainty exponent $\alpha \approx 0.7$. The truncated fractal Arnold tongues are present in the case of high dissipation as well, while the intermingled fractal pattern gradually disappears with increasing dissipation. [S1063-651X(98)04002-1]

PACS number(s): 05.45.+b, 47.53.+n, 47.54.+r

I. INTRODUCTION

During the past decade much attention has been paid to the investigation of a sensitive dependence, associated with the chaotic behavior of nonlinear dynamical systems, in phase space and in parameter space. The chaotic behavior of nonlinear dynamical systems is characterized in the phase space by two types of sensitive dependence on initial conditions. The first type is characterized by a positive Lyapunov exponent, i.e., by exponential separation of trajectories originating from neighboring initial conditions. The second type of sensitive dependence was found by Grebogi, McDonald, Ott, and Yorke [1]: a sensitive dependence of asymptotic attractors for systems with fractal basin boundaries [1–5]. Systems with multiple attractors can also exhibit an extreme type of fat fractals: the riddled basins [6–11]; in such cases the chaotic attractor is riddled with holes that belong to the basins of other attractors.

On the other hand, a sensitive dependence in parameter space was investigated by Farmer [12] using a logistic map. It was shown that the chaotic parameter set, i.e., the set of control parameter values generating chaotic attractors, is an example of a fat fractal, i.e., a fractal set with positive Lebesgue measure and box-counting dimension one [12,13]. In a further development, Lai and Winslow [14] found riddled chaotic parameter sets in spatiotemporal dynamical systems, implying an extreme sensitive dependence on parameters.

In this paper we investigate in parameter space and in phase space a sensitive dependence associated with periodic attractors in the absence of chaotic behavior. To this end we study first a single-well Duffing oscillator at weak forcing and low dissipation. In that region of parameter space there are no chaotic tongues. However, we find an interesting pattern of multiply intermingled Arnold tongues that are fat fractals associated with a weak dependence on parameters. It should be pointed out that this pattern is not related to the appearance of sustained chaos.

Extending the investigation to higher dissipation, we find that the pattern of truncated fractal Arnold tongues is present even at high dissipation, while the pattern of intermingled fractal Arnold tongues gradually disappears with increasing dissipation. The single-well Duffing oscillator

$$\ddot{x} + \gamma \dot{x} + x + x^3 = f \cos \omega t \quad (1)$$

has been investigated previously in the limits of strong dissipation [15–23] and in the Hamiltonian case [24].

On the other hand, it should be noted that, in general, investigations of low-dimensional dynamical systems at low dissipation have been scarce. It was shown recently that a periodically kicked mechanical rotor at small damping possesses a large number of coexisting periodic attractors and closely interwoven basins of attraction [25]. For a nonlinear oscillator with dry friction it was shown that a complex pattern of Arnold tongues at smaller and smaller scales appears for weak dissipation [26].

The Duffing oscillator (1) is characterized by the interplay of two frequencies: the dressed intrinsic frequency ω'_0 and the forcing frequency ω [16,17]. At low forcing f and weak dissipation γ , considered in this paper, we have periodic transients with entrainment of the forcing frequency to the dressed intrinsic frequency or quasiperiodic transients associated with irrational winding number $W = \omega/\omega'_0$. All these transients asymptotically approach the periodic attractors, which are characterized by a rational winding numbers $W = p/q$ (p, q are prime numbers). It is standard to refer to parameter regions of p/q entrainment as Arnold tongues [27].

The classic pattern of Arnold tongues in the forcing amplitude–forcing frequency parameter plane is associated with the sine circle map. In that case the p/q Arnold tongues are ordered through the Farey construction, where to each rational winding number p/q corresponds to one simple hornlike Arnold tongue [28].

II. FRACTAL AND TRUNCATED FRACTAL ARNOLD TONGUES AT LOW DISSIPATION

Let us first calculate Arnold tongues for the Duffing oscillator (1) at very low dissipation $\gamma = 0.001$ and for fixed initial conditions $x_0 = 0, \dot{x}_0 = 0$. In the first step each point on a 150×150 grid, with forcing frequency ω and forcing amplitude f given by the horizontal and vertical axes, respectively, was followed numerically to determine the asymptotic attractor.

In this way we obtain the diagram shown in Fig. 1. With increasing forcing there appear consecutive narrow tongues of period 2, 3, 5, 7, etc. At the point in parameter space with

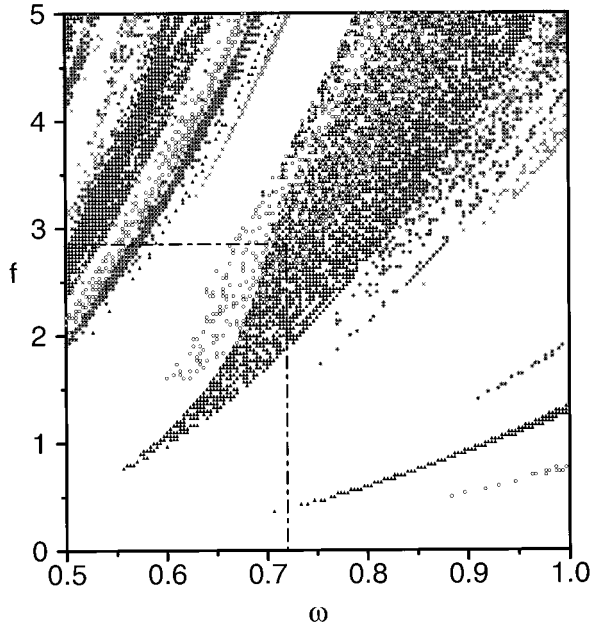


FIG. 1. Values of parameters f and ω that lead to periodic attractors of period 1 (blank), 2 (\circ), 3 (\blacktriangle), 4 (\diamond), 5 ($*$), 6 (∇), and 7 (\times) in the parameter region $0.5 \leq \omega \leq 1$ and $0 \leq f \leq 5$ (sampled over a uniform grid of 150×150 for the Duffing oscillator) (1) at low dissipation $\gamma = 0.001$. Fixed initial conditions $x_0 = 0, \dot{x}_0 = 0$ are used.

$\omega \approx 0.55, f \approx 0.7$ there is a tip of a broad period-3 tongue (closed triangles); above it, at $\omega \approx 0.6, f \approx 1.5$, there is a tip of a period-2 tongue (open circles). These two tongues intertwine above $\omega \approx 0.65, f \approx 1.7$. On the other hand, each of these tongues has holes that correspond to period 1. Thus, in the region around $\omega \approx 0.7, f \approx 2.5$ we have an intertwining of three tongues corresponding to the periods 1–3.

Let us now investigate in more details this region of ω, f parameter space. In particular we focus our attention on a small region of parameter plane defined by $0.7198 < \omega < 0.7203$ and $2.846 < f < 2.854$. The $\frac{2}{2}$, $\frac{3}{3}$, and $\frac{1}{1}$ Arnold tongues calculated in this parameter region on a 400×250 grid are displayed in Figs. 2(a), 2(b), and 2(c), respectively. Here a black dot was plotted on each grid point leading to an asymptote having a certain value of the winding number $W = p/q$, while no dot was plotted for grid points leading to attractors with other values of the winding number. These results show that a fine-scale intermingled structure is present in the parameter space, with two types of Arnold tongue pattern.

On a small scale, the $\frac{2}{2}$ Arnold tongue consists of many narrow black and blank parallel strips. However, a magnification of a portion of parameter space shows that this fractal-like pattern is truncated at some scale [Fig. 2(a)], so that further magnification displays smooth boundaries of this linear striated structure, without a repeated birth of new striations. We note that in Fig. 1(a) one strip of the $\frac{2}{2}$ Arnold tongue splits into two strips, which belong to the same winding number $\frac{2}{2}$ and to the same attractor. [All the strips in Fig. 1(a) belong to two existing asymptotic attractors of period 2.]

On the other hand, quite a different fractal pattern is obtained in the blank regions between the strips of the $\frac{2}{2}$ Arnold

tongues in Fig. 2(a); in these regions we obtain the intermingled fractal Arnold tongues having winding numbers $\frac{3}{3}$ [Fig. 2(b)] and $\frac{1}{1}$ [Fig. 2(c)]. In these cases the fine-scale structure is present on all scales (within computer precision), as revealed by illustrative magnifications of successively smaller and smaller regions of parameter space, which contain fine scale structure near the opening of the above-mentioned segment of the $\frac{1}{1}$ Arnold tongue at the place of splitting of the $\frac{2}{2}$ Arnold tongue [Figs. 2(d) and 2(e)]. Thus the $\frac{1}{1}$ Arnold tongues have a fractal-like structure, which geometrically resembles a form of classic chaotic strange attractor. Moreover, such fractal structures of the $\frac{1}{1}$ and $\frac{3}{3}$ Arnold tongues are intermingled at all scales, i.e., the fractal regions belonging to these two Arnold tongues are finely interwoven.

The appearance of a fractal pattern is usually considered as a strong indicator of chaotic motion [16] or of nonchaotic strange attractors [2], while here it appears for low-period Arnold tongues. We note that it was shown previously that for Duffing oscillators at rather low forcing amplitude and strong dissipation fractal basin boundaries appear [16,20]. On the other hand, a pattern with repeated births of striations under transformation of scale was previously found for basin boundaries in a transiently driven pendulum system [4].

Let us now investigate the sensitivity of Arnold tongues in Fig. 2 on parameters. In the previous investigations the sensitive dependence of chaotic parameter sets was quantified by the uncertainty exponent α [1,2]. In an analogous way we quantify the sensitive parameter dependence for the intermingled Arnold tongues in Fig. 2. To this end we proceed as follows. A set of values of forcing amplitude is drawn from a uniform distribution along a line of fixed frequency in Fig. 2(a). Consider only those N_t points from this distribution that lie on a $\frac{2}{2}$ Arnold tongue and denote each of the corresponding values of the forcing amplitude by f . In each case define $f' = f + \epsilon$, where ϵ is a small perturbation. Determine whether f' asymptotically approaches an Arnold tongue having a winding number different from $\frac{2}{2}$; in such a case this value of the parameter f is uncertain. This process is repeated for all N_t values of f , while holding the magnitude of perturbation ϵ unchanged. Assume that among these N_t values there are N_u uncertain parameter values. The fraction of uncertain parameter values of the forcing amplitude at perturbation ϵ for the $\frac{2}{2}$ Arnold tongues is then $P(\frac{2}{2}, \epsilon) = N_u / N_t$. By increasing ϵ the value of N_t increases until N_u reaches 400.

This process is then repeated at different values of the perturbation ϵ . Obviously, in analogy to [2], a small error ϵ in the system parameter f might alter the location of the basin boundary so that fixed initial conditions $x_0 = 0, \dot{x}_0 = 0$ cause a shift from one basin to another. In a similar way we determine the fractions $P(\frac{3}{3}, \epsilon)$ and $P(\frac{1}{1}, \epsilon)$ corresponding to Figs. 2(b) and 2(c), respectively.

In analogy to the chaotic case [1,2], one may expect that, if the basin boundary dimension is approximately constant in the region of parameter space being examined, the scaling of $P(p/q, \epsilon)$ is the same as the scaling of uncertainty fraction in the phase space, i.e.,

$$P\left(\frac{p}{q}, \epsilon\right) \sim \epsilon^{\alpha(p/q)}, \quad (2)$$

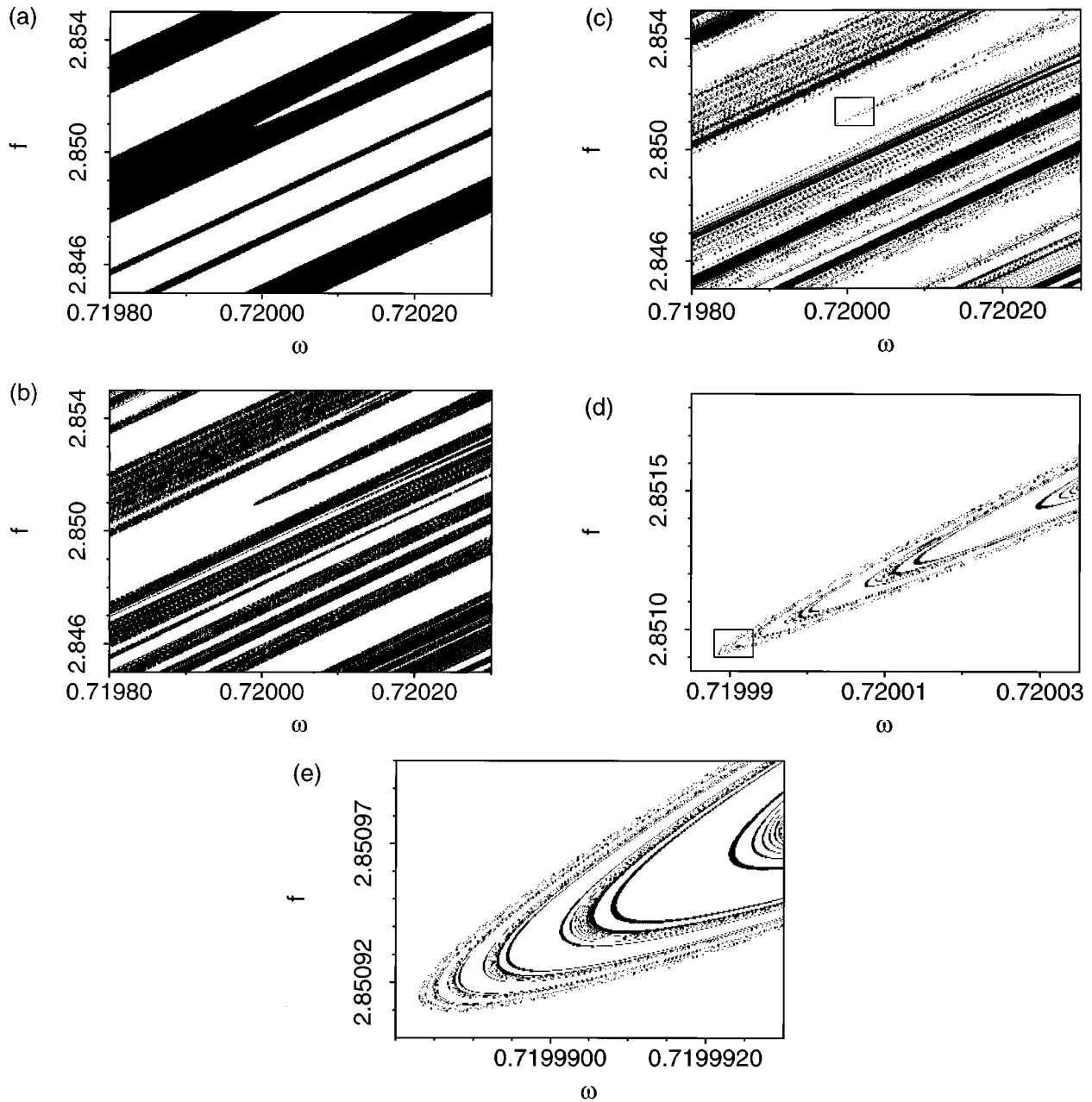


FIG. 2. Blowup of Fig. 1 over the parameter region $0.7198 < \omega < 0.7203$ and $2.845 < f < 2.855$ for (a) $\frac{2}{3}$ Arnold tongues (black dots), (b) $\frac{3}{3}$ Arnold tongues (black dots), and (c) $\frac{1}{1}$ Arnold tongues (black dots). (d) and (e) Two successively expanded views of a detail of the $\frac{1}{1}$ Arnold tongues. No other Arnold tongues were found in the above parameter region.

where $\alpha(p/q)$ is the uncertainty exponent associated with the p/q Arnold tongue. Calculating α at the frequency $\omega = 0.7199895$, i.e., which is a sweep through the opening of the above intermingled $\frac{1}{1}$ and $\frac{3}{3}$ Arnold tongue fractal structures, we obtain the uncertainty exponent $\alpha \approx 0.7$ for the $\frac{1}{1}$ and $\frac{3}{3}$ Arnold tongues. As expected, for the $\frac{2}{2}$ Arnold tongue the uncertainty exponent is close to 1, $\alpha \approx 1.0$.

Calculating the uncertainty exponent α for different subsets of (ω, f) parameter space in Fig. 2 we have found that roughly the same value $\alpha \approx 0.7$ corresponds to the $\frac{1}{1}$ and $\frac{3}{3}$ Arnold tongues everywhere in the parameter space of Fig. 2 and the other value $\alpha \approx 1.0$ to the $\frac{2}{2}$ Arnold tongue. This result can be compared to the previous results obtained for the chaotic basin structure of the kicked double rotor that the

uncertainty coefficient α takes one value in the subregion that is fractal and the other (integer) in the subregion that is not fractal, with both subregions being intertwined [3].

Obviously, the fractal Arnold tongues discussed above reflect the fractal-like structure of basin boundaries in phase space. To show this we have constructed a relevant section of phase space around the fixed initial conditions $x_0 = 0, \dot{x}_0 = 0$, performing the calculation for parameter values $f = 2.85092, \omega = 0.71999$, which correspond to a point in parameter space near the tip of the $\frac{1}{1}$ Arnold tongue in Figs. 2(d) and 2(e). We take a grid of initial conditions $-0.05 < x_0 < 0.05, -0.05 < \dot{x}_0 < 0.05$ around the initial point $x_0 = 0, \dot{x}_0 = 0$ used in the calculations from Fig. 2. In this way we obtain the basins of attraction of periods 1–3, shown

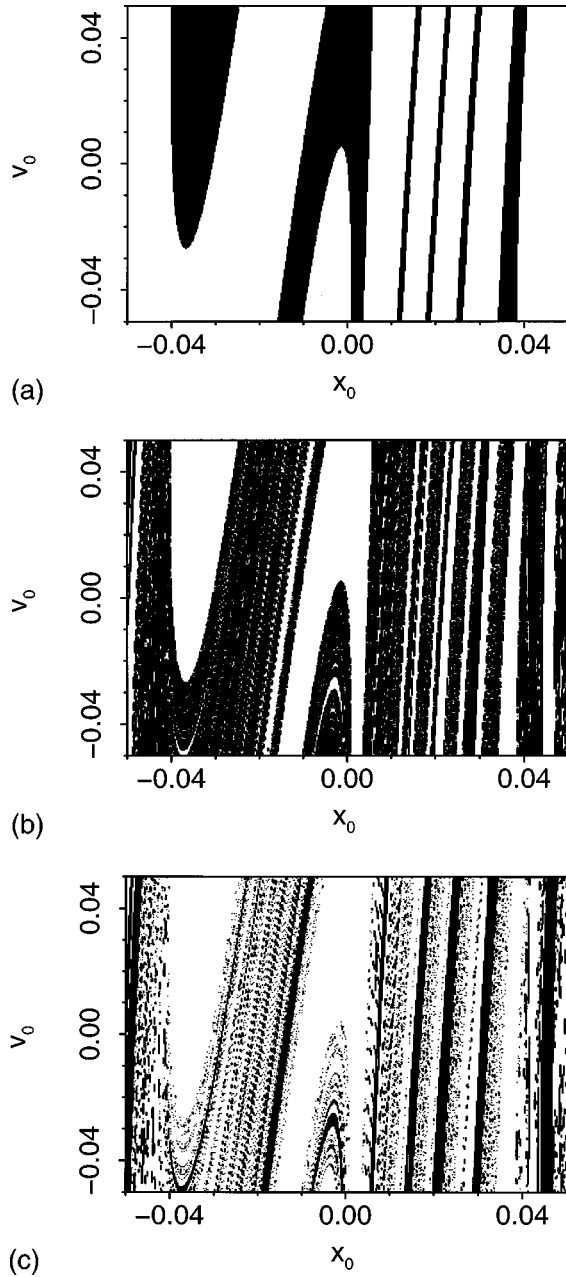


FIG. 3. Basins of attraction for the single-well Duffing oscillator (1) at low dissipation $\gamma=0.001$ in the initial condition region $-0.05 \leq x_0 \leq 0.05$ and $-0.05 \leq \dot{x}_0 \leq 0.05$ for the parameters $\omega = 0.71999$ and $f = 2.85092$: (a) period-2 basins, (b) period-3 basins, and (c) period-1 basins.

in Fig. 3. These basins of attraction are associated with five asymptotic attractors, two of period 1, two of period 2, and one of period 3 (Fig. 4). We were not able to find any other attractor in the phase space. Because of the rather small forcing amplitude in the present calculations, the number of attractors is rather small (5) in the region being closely investigated, although the dissipation is low. It is well known that, in general, the number of asymptotic attractors in dissipative systems increases with lowering dissipation, approaching infinity in the Hamiltonian limit [2,25]. This trend is also seen for the Duffing oscillator (1) by further decreasing the value of dissipation strength γ below 0.001.

As seen from Fig. 3, the basins of attraction of period 1, 2,

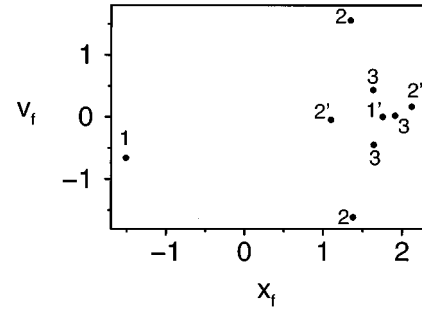


FIG. 4. Attractors of the Duffing oscillator (1) for the parameter values $\gamma=0.001$, $\omega=0.71999$, and $f=2.85092$ of period 1 (denoted 1 and 1'), 2 (denoted 2 and 2'), and 3 (denoted 3). No other attractors were found.

and 3 correspond to the $\frac{1}{1}$, $\frac{2}{2}$, and $\frac{3}{3}$ Arnold tongues in Fig. 1, respectively. Consequently, the values of the uncertainty exponent are $\alpha \approx 0.7$ for the intermingled period-1 and period-3 basins and $\alpha \approx 1.0$ for the period-2 basin with a truncated fractal boundary. These values are practically the same as for the corresponding Arnold tongues in Fig. 2. This is in accordance with the general expectation that the uncertainty exponents computed in phase space and parameter space are equivalent, in analogy to the previous study of chaotic spatiotemporal systems [14].

III. TRUNCATED FRACTAL ARNOLD TONGUES AT HIGH DISSIPATION

Let us now investigate the question whether the intermingled Arnold tongues appear at high dissipation. To this end we perform a sequence of calculations in the region of overlap of the major $\frac{2}{2}$ and $\frac{3}{3}$ Arnold tongues with increasing dissipation strength. In general, we find that with increasing

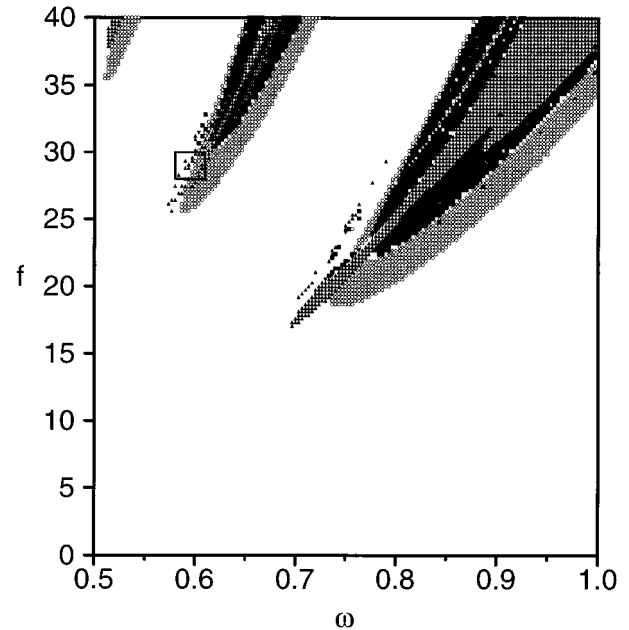


FIG. 5. Values of the parameters f and ω that lead to periodic attractors (denoted the same way as in Fig. 1) and to chaotic attractors (■) for the Duffing oscillator (1) at high dissipation $\gamma=0.2$. Fixed initial conditions $x_0=0$ and $\dot{x}_0=0$ are used.

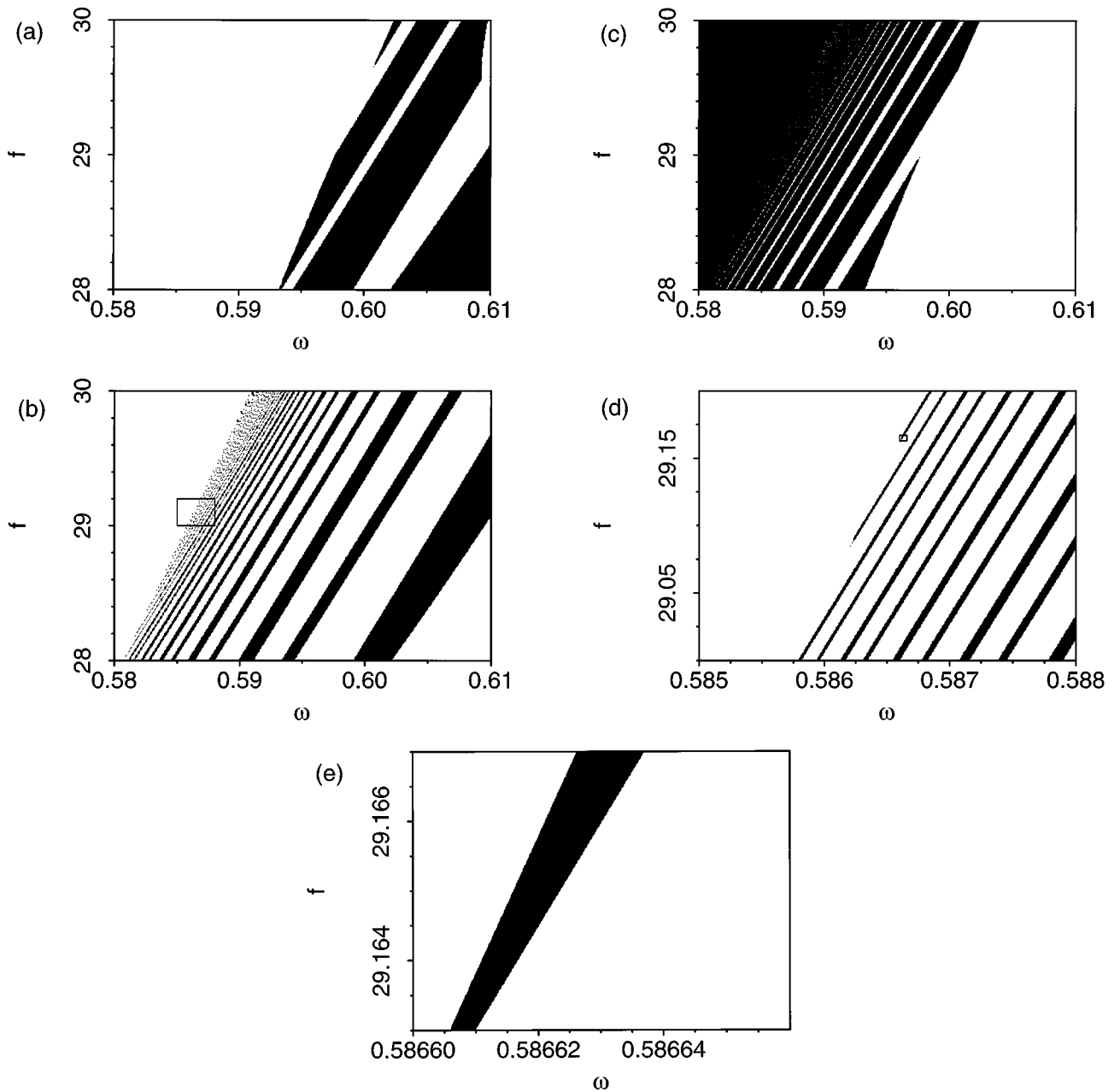


FIG. 6. Blowup of Fig. 5 over the parameter region $0.58 \leq \omega \leq 0.61$ and $28 \leq f \leq 30$ for (a) $\frac{2}{2}$ Arnold tongues (black dots), (b) $\frac{3}{3}$ Arnold tongues (black dots), and (c) $\frac{1}{1}$ Arnold tongues (black dots). (d) and (e) Two successively expanded views of a detail of the $\frac{3}{3}$ Arnold tongues.

dissipation the uncertainty exponent α in the overlap region gradually increases towards 1 and for a high dissipation $\gamma = 0.2$ we obtain $\alpha \approx 1.0$ for $\frac{2}{2}$ and $\frac{3}{3}$ Arnold tongues.

In Fig. 5 we present for high dissipation $\gamma = 0.2$ the state diagram in parameter space, in analogy to Fig. 1. In the frequency interval $0.5 \leq \omega \leq 1$ there are three major tongues. In comparison to Fig. 1 the tips of these tongues are shifted towards higher forcing strengths. The second feature is that the chaotic tongues (closed squares) are closer to the tips of Arnold tongues than in the case of weak dissipation.

In analogy to our previous considerations of the low dissipation case (Fig. 2), let us now focus our attention on a small region of parameter plane defined by $0.58 \leq \omega \leq 0.61$ and $28 \leq f \leq 30$, where the $\frac{2}{2}$ and $\frac{3}{3}$ Arnold tongues overlap (the tongue in the middle of Fig. 5). The $\frac{2}{2}$, $\frac{3}{3}$, and $\frac{1}{1}$ Arnold

tongues in that region of parameter plane are displayed in Figs. 6(a), 6(b), and 6(c), respectively. Two successively expanded views of a detail of the $\frac{3}{3}$ Arnold tongues are shown in Figs. 6(d) and 6(e). We find that the pattern of truncated fractal Arnold tongues is present in the case of high dissipation as well, but not the pattern of intermingled fractal Arnold tongues.

IV. CONCLUSION

In this paper we investigate the fractal pattern of Arnold tongues associated with the single-well Duffing oscillator in the parameter region without sustained chaotic behavior. In particular we study the overlapping region of the $\frac{2}{2}$ and $\frac{3}{3}$ Arnold tongues in the case of weak dissipation and we find

an exotic parameter space structure of Arnold tongues of two types: the truncated fractal type (for the $\frac{2}{3}$ Arnold tongues) and the intermingled fractal type (for the $\frac{1}{3}$ and $\frac{2}{3}$ Arnold tongues). These structures exhibit a weak type of sensitive dependence of asymptotic attractors on parameters that distinguish between Arnold tongues having different winding numbers. Namely, for the $\frac{1}{3}$ and $\frac{2}{3}$ Arnold tongues the uncertainty exponent is $\alpha \approx 0.7$, implying the exterior dimension $d_{ex} = D - \alpha = 1.3$. Assuming, for example, that the parameter f can be determined to a precision of 10^{-14} , then $P(\epsilon) \sim (10^{-14})^{0.7} \sim 10^{-10}$ and hence the probability of error in the numerical prediction of the final-state Arnold tongue is roughly 1 in 10^{10} . This means that in the case considered here, in spite of an exotic fractal-like structure, the computer simulations are quite reliable, i.e., the dependence of asymptotic attractors on system parameters is very weak, weaker than in the case of the chaotic parameter set associated with the logistic map having $\alpha \approx 0.4$ [1,12]. However, by a further reduction of dissipation, a more and more sensitive dependence of asymptotic attractors on system parameters will appear, leading to a pattern of Arnold tongues with an extremely sensitive dependence.

One might speculate on a possible origin of fractal Arnold tongue structure in the parameter region that is far removed from the regions with chaotic behavior. We note that such behavior might be related to the appearance of transient cha-

otic behavior of the system before it settles down in one of the periodic attractors. Namely, the sensitive dependence of the lifetime of the chaotic transient on initial conditions and parametrization may be associated with the appearance of fractal boundaries. Thus the fractal Arnold tongues might be considered as identifying characteristics of transient chaos.

On the other hand, with an increase of dissipation strength the uncertainty exponent associated with Arnold tongues gradually approaches unity, i.e., the intermingled pattern of fractal Arnold tongues disappears. However, the truncated fractal Arnold tongues appear even in the case of high dissipation.

As for the generality of our results on intermingled fractal Arnold tongues, it seems that they appear as a general pattern associated with weak dissipation. The appearance of intermingled fractal Arnold tongues is not restricted only to a segment of the parameter space being considered, but is associated with other regions of the parameter space too. For example, we find a similar pattern for the intermingled Arnold tongues of periods 4 and 7 around $\omega \approx 6.61$, $f \approx 37.6$, and $\gamma = 5 \times 10^{-4}$. Furthermore, in preliminary calculations we have found that this pattern is not restricted to the Hamiltonian (1), but is of a more general character. For example, we find a similar pattern for oscillators with different types of dissipation, including weak quadratic and Coulomb damping.

-
- [1] C. Grebogi, S. W. McDonald, E. Ott, and J. A. Yorke, Phys. Lett. **99A**, 415 (1983); S. W. McDonald, C. Grebogi, E. Ott, and J. A. Yorke, Physica D **17**, 125 (1985).
- [2] E. Ott, *Chaos in Dynamical Systems* (Cambridge University Press, Cambridge, 1993).
- [3] C. Grebogi, E. Kostelich, E. Ott, and J. A. Yorke, Physica D **25**, 347 (1987).
- [4] M. Varghese and J. S. Thorp, Phys. Rev. Lett. **60**, 665 (1988).
- [5] C. Bleher, C. Grebogi, E. Ott, and R. Brown, Phys. Rev. A **38**, 930 (1988).
- [6] J. C. Alexander, J. A. Yorke, Z. You, and J. Kan, Int. J. Bifurcation Chaos **2**, 795 (1992).
- [7] E. Ott, J. C. Sommerer, J. C. Alexander, J. Kan, and J. A. Yorke, Phys. Rev. Lett. **71**, 4134 (1993); E. Ott, J. C. Alexander, J. Kan, J. C. Sommerer, and J. A. Yorke, Physica D **76**, 384 (1994).
- [8] J. F. Heagy, T. L. Carroll, and L. M. Pecora, Phys. Rev. Lett. **73**, 3528 (1994).
- [9] Y. C. Lai and C. Grebogi, Phys. Rev. E **54**, 2489 (1996).
- [10] M. Ding and W. Yang, Phys. Rev. E **54**, 2489 (1996).
- [11] Y. C. Lai, C. Grebogi, J. A. Yorke, and S. C. Venkataramani, Phys. Rev. Lett. **77**, 55 (1996).
- [12] J. D. Farmer, Phys. Rev. Lett. **55**, 351 (1985).
- [13] D. K. Umberger and J. D. Farmer, Phys. Rev. Lett. **55**, 661 (1985).
- [14] Y. C. Lai and R. L. Winslow, Phys. Rev. Lett. **72**, 1640 (1994); Physica D **74**, 353 (1994).
- [15] C. Duffing, *Erzwungene Schwingungen bei Veränderlicher Eigenfrequenz und ihre Technische Bedeutung* (Vieweg, Braunschweig, 1918).
- [16] F. S. Moon, *Chaotic Vibrations* (Wiley, New York, 1987).
- [17] M. Lakshamanan and K. Murali, *Chaos in Nonlinear Oscillators* (World Scientific, Singapore, 1996).
- [18] Y. Ueda, J. Stat. Phys. **20**, 181 (1979).
- [19] U. Parlitz and W. Lauterborn, Phys. Lett. **107A**, 351 (1985).
- [20] C. Pezeshki and E. H. Dowell, Physica D **32**, 194 (1988).
- [21] E. Kreuzer, M. Kleczke, and S. Schaub, Chaos Solitons Fractals **1**, 439 (1991).
- [22] C. L. Olsson and M. G. Olsson, Am. J. Phys. **59**, 907 (1991).
- [23] F. Xie and G. Hu, Phys. Rev. E **51**, 2773 (1995).
- [24] M. Bier and T. C. Bountis, Phys. Lett. **104A**, 239 (1984).
- [25] U. Feudel, C. Grebogi, B. R. Hunt, and J. A. Yorke, Phys. Rev. E **54**, 71 (1996).
- [26] V. Paar, N. Pavin, N. Paar, and B. Novaković, Robotica **14**, 423 (1996).
- [27] J. W. Norris, Nonlinearity **6**, 1093 (1993).
- [28] M. H. Jensen, P. Bak, and T. Bohr, Phys. Rev. A **30**, 1960 (1984).